

Copyright 2003 IEEE. Published in the Proceedings of the  
Hawaii International Conference On System Sciences,  
January 5-8, 2003, Big Island, Hawaii

# Coordinated Interchange Scheduling and Opportunity Cost Payment: A Market Proposal to Seams Issues

Jie Chen\*  
[jc227@cornell.edu](mailto:jc227@cornell.edu)

James S. Thorp\*  
[jst6@cornell.edu](mailto:jst6@cornell.edu)

Timothy D. Mount#  
[tdm2@cornell.edu](mailto:tdm2@cornell.edu)

\* *School of Electrical & Computer Engineering, Cornell University*

# *Dept. of Applied Economics & Management, Cornell University*

## Abstract

*This paper presents a joint market structure for energy, spinning reserves and VAR support in a multi-area setting. It is based on a co-optimization that can simultaneously optimize all three commodities across the “seams”. An auxiliary problem principle based decomposition scheme is applied to the overall optimization for coordinating interchanges of energy and ancillary services between control areas. The proposed decomposition approach preserves independent dispatching for neighboring areas while achieves overall optimum. Nodal prices for energy and opportunity cost payments to forgone energy profit due to providing reserves and VAR support are also addressed. We believe the algorithm is of particular interest in the restructuring electricity industry for resolving seams issues. An illustrative example of a modified IEEE 30-bus system is used to demonstrate the validity of proposed algorithm.*

## 1. Background

The term “seam” has come into common use recently in the restructuring electric industry to refer to a boundary between neighboring control areas or power markets. Seams issues may be characterized as the difficulties of conducting power transactions across the boundary due to differences in operating rules and market designs, as well as differences in business practices. They include diverse matters such as different bidding rules, different pricing mechanisms, inconsistent transaction submittal times, or different operating procedures. Even apparently minor differences in rules can create seams problems. Such is the case among the Northeastern ISOs, although their market designs and transmission congestion management systems are substantially similar. An extensive list of seams issues and ISO rule differences among these ISOs is available at the ISO Memorandum of Understanding website [1]. Seams problems inhibit competition in the power markets, result in inefficient market practice and

sometimes may expose market participants to considerable financial risks.

The resolution of inter-regional seams issues can reduce trading barriers between electricity markets and advance competition. More choices together with enhanced trading flexibility will then be offered to market participants. Market participants have long called for a “seamless” market. FERC also has signaled the commission’s inclination, through several orders and SMD NOPR, towards more coordination and uniformity of business models and practices among the various ISOs. Several efforts are underway within the industry to address seams problems and the development of standards. A specific example of these efforts is a Memorandum of Understanding among several Northeast ISOs [1], through which major inter-regional seams issues have been identified and prioritized. Also in 2002, the Northeastern Independent Market Operators Coordinating Committee [2] was formed among three ISOs (NYISO, ISO-NE, and IMO) to work towards solutions of a host of seams and market standardization issues.

Eliminating seams is a challenging process that may take many years to accomplish. First of all, the goal is to make power markets more similar or *standardized* in order to reduce trading barriers. Three Northeastern ISOs have struggled to coordinate their rules to lower trading barriers but have only achieved limited success after several years [3]. Secondly, it requires the coordination of net exchange between neighboring ISOs. It involves the coordination of the energy flow and payments between ISOs as well as the coordination of ancillary service requirements and characterizations needed for grid management. Market standardization issues are beyond the scope of this paper. Instead, the interchange coordination is our focus here, assuming no trading barriers exist.

Most of the existing LMP based markets currently utilize proxy bus mechanisms to represent and value inter-regional exchanges. Simply put, the proxy bus models the location at which *marginal* changes in generation are

assumed to occur in response to changes in inter-regional transactions. Nevertheless, as Harvey pointed out [4], a proxy bus system can fail to produce the optimal level of net interchange and may jeopardize the overall efficiency of the market if the number and location of the proxy buses are not appropriately chosen. Unfortunately, the selection of proxy buses to reflect the actual *marginal* generation location to support inter-regional transactions is not an easy nut to crack. It involves a variety of considerations and there are still open questions to be answered [4].

In essence, the ultimate goal of coordinating interchange between regions is trying to achieve the overall system optimum while preserving independent optimal dispatch for each of the connected regions. This has much in common with decomposition approaches for solving large-scale optimization problems. Kim and Baldick pioneered the related work for the large-scale distributed OPF [5-7], in which the overall OPF problem was decomposed into several regions through an iterative update on constraint Lagrange multipliers. Although their focus was on the implementations for the parallel OPF computing, their results have implications for market coordination. Another relevant work is [8], in which Hogan et al. proposed a similar decomposition approach while in the market setting to tackle the transmission loading relief problem across multiple regions. Even though their work is not directly towards seams issues, their experience gives reason for optimism for resolving seams coordination via the same regional decomposition approach.

Presented in this paper is our attempt to coordinate energy as well as ancillary services, in particular, spinning reserves and VAR support, across the seams. The proposed market has a joint market structure based on a co-optimization that can simultaneously optimize energy and ancillary services. The same decomposition principle as in [5-8] is applied to coordinate the inter-regional exchanges. The LMP for energy is derived in the co-optimization setting. Opportunity cost payments to forgone energy profit due to providing ancillary services are also discussed.

## 2. Optimization Framework and Decomposition Schemes

The coordination of energy and ancillary services is based on a co-optimization (CO-OPT) framework first introduced in [9-10]. A quick review of the formulation for the overall system is provided in the following section. Then the decomposition approach is conceptually illustrated step by step through simple examples. The regional decomposition for a multi-area OPF is introduced

first, followed by the system decomposition approach for multiple system cases in a single-region CO-OPT setting, and finally we present the way to decompose the combined system — multi-area multi-system CO-OPT. The general and formal decomposition formulation is given later in Appendix A.

### 2.1. Notation

In this paper the following notation will be used. Additional symbols will be introduced when necessary.

$i$ :	generator index ( $i = 1, 2, \dots, I$ )
$j$ :	bus index ( $j = 1, 2, \dots, J$ )
$l$ :	transmission line index ( $l = 1, 2, \dots, L$ )
$k$ :	contingency index ( $k = 0, 1, \dots, K$ ), 0 indicates the base case (intact system), predefined contingencies otherwise.
$P_{ik} / Q_{ik}$ :	real/reactive power output of generator $i$ in the $k^{\text{th}}$ contingency.
$R_{ik}$ :	spinning reserve carried by generator $i$ in the $k^{\text{th}}$ contingency.
$\theta_{jk}$ :	voltage angle of bus $j$ in the $k^{\text{th}}$ contingency.
$V_{jk}$ :	voltage magnitude of bus $j$ in the $k^{\text{th}}$ contingency.
$S_{lk}$ :	power flow of line $l$ in the $k^{\text{th}}$ contingency.
$P_i^{\min}, P_i^{\max}$ :	minimum and maximum real power capacity for generator $i$
$Q_i^{\min}, Q_i^{\max}$ :	minimum and maximum reactive power capacity for generator $i$
$R_i^{\max}$ :	maximum reserve for generator $i$
$V_j^{\min}, V_j^{\max}$ :	voltage magnitude limits for bus $j$
$S_l^{\max}$ :	power flow limit for line $l$
$C_{P_i}(P_{ik})$ :	energy cost for operating generator $i$ at output level $P_{ik}$ in the $k^{\text{th}}$ contingency.
$C_{R_i}(R_{ik})$ :	reserve cost for generator $i$ carrying $R_{ik}$ spinning reserve in the $k^{\text{th}}$ contingency.
$p_k$ :	the probability of the $k^{\text{th}}$ contingency

### 2.2. Overview of CO-OPT formulation

The CO-OPT framework [9-10] is utilized to optimize energy and spinning reserves simultaneously.

In brief, the CO-OPT is to minimize the total expected cost over the predefined base case and credible contingencies,

$$\min_{P, R} \sum_{k=0}^K p_k \left\{ \sum_{i=1}^I [C_{P_i}(P_{ik}) + C_{R_i}(R_{ik})] \right\} \quad (1)$$

meanwhile subject to network and system constraints enforced by each of the base case and contingencies. These constraints include nodal power balancing constraints,

$$F_{jk}(\theta, V, P, Q) = 0, \quad j = 1, \dots, J \quad k = 0, \dots, K \quad (2)$$

line power flow constraints (detailed formulations for (2) and (3) are referred to [11]),

$$|S_{lk}| \leq S_l^{\max}, \quad l = 1, \dots, L \quad k = 0, \dots, K \quad (3)$$

voltage limits

$$V_j^{\min} \leq V_{jk} \leq V_j^{\max}, \quad j = 1, \dots, J \quad k = 0, \dots, K \quad (4)$$

generation limits

$$\begin{aligned} P_i^{\min} &\leq P_{ik} \leq P_i^{\max} \\ Q_i^{\min} &\leq Q_{ik} \leq Q_i^{\max}, \quad i = 1, \dots, I \quad k = 0, \dots, K \end{aligned} \quad (5)$$

spinning reserve ramping limits

$$0 \leq R_{ik} \leq R_i^{\max}, \quad i = 1, \dots, I \quad k = 0, \dots, K \quad (6)$$

and unit capacity limits

$$P_{ik} + R_{ik} \leq P_i^{\max}, \quad i = 1, \dots, I \quad k = 0, \dots, K \quad (7)$$

The concept of *Total Unit Committed Capacity (TUCC)* is introduced to build connections between the base case and contingencies. In particular, the TUCC of unit  $i$  in the  $k^{\text{th}}$  contingency is defined as

$$G_{ik} = P_{ik} + R_{ik}, \quad i = 1, \dots, I \quad k = 0, \dots, K \quad (8)$$

As indicated in [9], the TUCC for any generator  $i$  is required to be the same over all  $K+1$  cases, thereby is denoted as  $G_i^{\max}$ , and the following holds,

$$G_{ik_1} = G_{ik_2} = G_i^{\max}, \quad i = 1, \dots, I \quad k_1, k_2 = 0, \dots, K \quad (9)$$

### 2.3. Regional Distributed OPF

The purpose is to carefully decompose the overall OPF problem into geographical regions by introducing “dummy” variables at the border buses that mimic the effects of the external part of the system, and introducing constraints that they be equal at adjacent regions. By solving the optimal power flows for each region and coordinating them through iterative updates on the constrained Lagrange multipliers, the algorithm is shown to converge to a solution of the full OPF problem [5-7].

To illustrate the regional decomposition, consider Fig.1 where a power system consists of two regions (region A and region B) connected by one single tie-line. The variables within each region are denoted by  $x_A$  and  $x_B$  respectively, which are real and reactive power-flows through the buses and the voltages and phase angles at the buses. At the border, for the tie-line between the regions, a “dummy” bus is created and the associated variables for this bus are denoted by  $y$ .

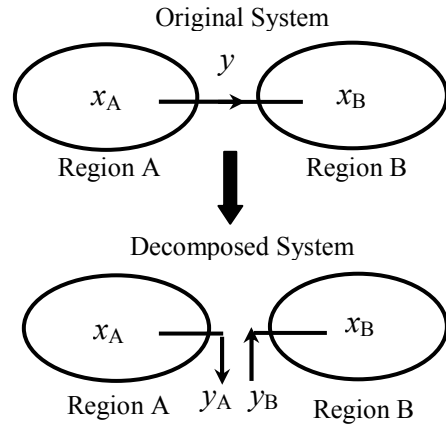


Figure 1. Example of regional OPF decomposition

The approach relies on decomposing the overall problem into regions by duplicating the border variables and imposing coupling constraints between the two copies. Hence, the “dummy” variables associated with region A are  $y_A$  while those associated with region B are  $y_B$ , and the coupling constraint is  $y_A = y_B$ . In summary, the state variables associated with the OPF for region A are  $(x_A, y_A)$  and the state variables associated with the OPF for region B are  $(x_B, y_B)$ . Hence, for  $\gamma \geq 0$ , the OPF problem for the overall system can be formally written as:

$$\min_{\substack{(x_A, y_A) \\ (x_B, y_B)}} \left\{ c_A(x_A) + c_B(x_B) + \frac{\gamma}{2} \|y_A - y_B\|^2 : y_A - y_B = 0 \right\} \quad (10)$$

where the quadratic term helps in the convergence of the solution but does not affect the solution as  $y_A = y_B$ .

By applying *Auxiliary Problem Principle (APP)*[12], the problem takes the following form:

$$\begin{aligned} \begin{pmatrix} x_A^{k+1}, y_A^{k+1} \\ y_B^{k+1}, x_B^{k+1} \end{pmatrix} &= \min_{\substack{(x_A, y_A) \\ (x_B, y_B)}} \left\{ \begin{aligned} &c_A(x_A) + c_B(x_B) + \\ &\frac{\beta}{2} \|y_A - y_A^k\|^2 + \frac{\beta}{2} \|y_B - y_B^k\|^2 + \\ &\gamma(y_A - y_B)^T (y_A^k - y_B^k) + \\ &\lambda^k (y_A - y_B) \end{aligned} \right\} \\ \lambda^{k+1} &= \lambda^k + \alpha(y_A^{k+1} - y_B^{k+1}) \end{aligned} \quad (11)$$

where  $k$  is the iteration index,  $\alpha, \beta, \gamma$  are positive constants.

Equivalently, the above problem can be decomposed into two independent sub-problems for region A and B, respectively, that can be solved by the following iterative scheme:

$$OPF_A: \begin{aligned} (x_A^{k+1}, y_A^{k+1}) &= \min_{(x_A, y_A)} \left\{ \begin{aligned} &c_A(x_A) + \frac{\beta}{2} \|y_A - y_A^k\|^2 \\ &+ \gamma y_A^T (y_A^k - y_B^k) + \lambda^k y_A \end{aligned} \right\} \end{aligned} \quad (12)$$

$$OPF_B: \begin{aligned} (x_B^{k+1}, y_B^{k+1}) &= \min_{(x_B, y_B)} \left\{ \begin{aligned} &c_B(x_B) + \frac{\beta}{2} \|y_B - y_B^k\|^2 \\ &+ \gamma y_B^T (y_B^k - y_A^k) - \lambda^k y_B \end{aligned} \right\} \end{aligned} \quad (13)$$

$$\begin{aligned} \text{Update } \lambda: \\ \lambda^{k+1} &= \lambda^k + \alpha(y_A^{k+1} - y_B^{k+1}) \end{aligned} \quad (14)$$

Among the four duplicated *boundary variables* (voltage magnitudes, phase angles, real and reactive powers), the duplication of phase angles deserves more attention. The reason is that, in the overall OPF problem there is only one global reference, however, there are as many references generated as the number of the subsystems in the decomposed problems. These references have to be assumed the right values against the global reference to achieve convergence. One possible way is that altering each reference at each iterate in a manner such that the average of the phase angles at the border buses of a region equals the corresponding ones in adjacent regions.

## 2.4. Distributed Co-optimization

The above described decomposition scheme applies for the CO-OPT also. Nevertheless, there are no physical “tie-lines” between the base case and contingencies. The “tie” here is the TUCC for each of the generators. Take Fig.2 as an example, for the simple matter, which assumes the CO-OPT is formulated for one single-region power

system with the base case and only one contingency case. The non-physical “ties” are represented by the dashed lines in the graph.

The state variables for the base case (case #0) and the contingency case (case #1) are denoted by  $x_0$  and  $x_1$  respectively. The tie variables, TUCC, are denoted by  $y$ . And the two copies  $y_0$  and  $y_1$  are assigned to each of the two cases with the coupling constraint  $y_0 = y_1$  for the purpose of decomposition.

Hence, the overall CO-OPT formulation and the decomposition iterative scheme for this example can be written as Equ. (10) ~ (14) with only subscripts changes. The subscripts ‘0’ and ‘1’ replace the subscripts ‘A’ and ‘B’ respectively.

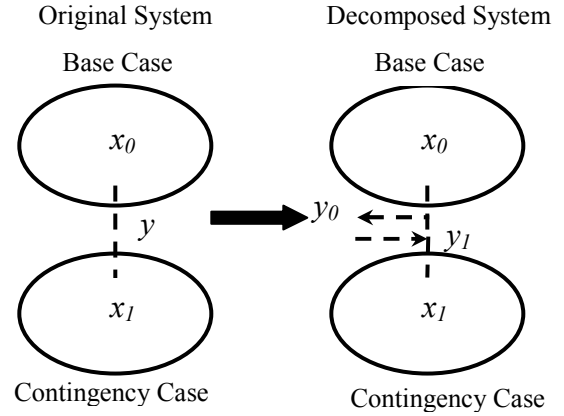


Figure 2. Example of the CO-OPT decomposition

## 2.5. Distributed Co-optimization Across Seams

Our ultimate goal is to do *Distributed Co-optimization Across Seams* (DCAS), by which the energy and ancillary services can be coordinated simultaneously between multiple regions. Apparently, the same decomposition concept works. What we need to do is to bundle up regional distributed OPF and distributed CO-OPT in the multiple-region setting. The iterations are not only over the collection of border “dummy” variables between multiple areas but also over the collection of generator TUCCs between the base case and all predefined contingencies. Fig. 3 depicts the simplest possible situation where a power system consists of two regions with only one contingency to worry about. The state variables are denoted by  $x_{0A}, x_{0B}, x_{1A}$  and  $x_{1B}$  for two areas and two cases respectively.  $y_0$  and  $y_1$  represent the physical “ties” between regions, while  $z_A$  and  $z_B$  represent the non-physical “ties” between cases.

The overall CO-OPT then can be decomposed into four independent sub-problems for each of the two regions in each of the two system conditions as follows:

$$\begin{aligned}
OPF_{0A}: \\
(x_{0A}^{k+1}, y_{0A}^{k+1}, z_{0A}^{k+1}) = \min_{(x_{0A}, y_{0A}, z_{0A})} \{ & p_0 \cdot c_{0A}(x_{0A}) \\
& + \beta_{0y} / 2 \|y_{0A} - y_{0A}^k\|^2 + \gamma_{0y} y_{0A}^T (y_{0A}^k - y_{0B}^k) + \lambda_{0y}^k y_{0A} \\
& + \beta_{Az} / 2 \|z_{0A} - z_{0A}^k\|^2 + \gamma_{Az} z_{0A}^T (z_{0A}^k - z_{1A}^k) + \lambda_{Az}^k z_{0A} \} \quad (15)
\end{aligned}$$

$$\begin{aligned}
OPF_{0B}: \\
(x_{0B}^{k+1}, y_{0B}^{k+1}, z_{0B}^{k+1}) = \min_{(x_{0B}, y_{0B}, z_{0B})} \{ & p_0 \cdot c_{0B}(x_{0B}) \\
& + \beta_{0y} / 2 \|y_{0B} - y_{0B}^k\|^2 + \gamma_{0y} y_{0B}^T (y_{0B}^k - y_{0A}^k) - \lambda_{0y}^k y_{0B} \\
& + \beta_{Bz} / 2 \|z_{0B} - z_{0B}^k\|^2 + \gamma_{Bz} z_{0B}^T (z_{0B}^k - z_{1B}^k) + \lambda_{Bz}^k z_{0B} \} \quad (16)
\end{aligned}$$

$$\begin{aligned}
OPF_{1A}: \\
(x_{1A}^{k+1}, y_{1A}^{k+1}, z_{1A}^{k+1}) = \min_{(x_{1A}, y_{1A}, z_{1A})} \{ & p_1 \cdot c_{1A}(x_{1A}) \\
& + \beta_{1y} / 2 \|y_{1A} - y_{1A}^k\|^2 + \gamma_{1y} y_{1A}^T (y_{1A}^k - y_{1B}^k) + \lambda_{1y}^k y_{1A} \\
& + \beta_{Az} / 2 \|z_{1A} - z_{1A}^k\|^2 + \gamma_{Az} z_{1A}^T (z_{1A}^k - z_{0A}^k) - \lambda_{Az}^k z_{1A} \} \quad (17)
\end{aligned}$$

$$\begin{aligned}
OPF_{1B}: \\
(x_{1B}^{k+1}, y_{1B}^{k+1}, z_{1B}^{k+1}) = \min_{(x_{1B}, y_{1B}, z_{1B})} \{ & p_1 \cdot c_{1B}(x_{1B}) \\
& + \beta_{1y} / 2 \|y_{1B} - y_{1B}^k\|^2 + \gamma_{1y} y_{1B}^T (y_{1B}^k - y_{1A}^k) - \lambda_{1y}^k y_{1B} \\
& + \beta_{Bz} / 2 \|z_{1B} - z_{1B}^k\|^2 + \gamma_{Bz} z_{1B}^T (z_{1B}^k - z_{0B}^k) - \lambda_{Bz}^k z_{1B} \} \quad (18)
\end{aligned}$$

The iterative procedure is coordinated by the updates of Lagrange multipliers:

$$\lambda_{0y}^{k+1} = \lambda_{0y}^k + \alpha_{0y} (y_{0A}^{k+1} - y_{0B}^{k+1}) \quad (19)$$

$$\lambda_{1y}^{k+1} = \lambda_{1y}^k + \alpha_{1y} (y_{1A}^{k+1} - y_{1B}^{k+1}) \quad (20)$$

$$\lambda_{Az}^{k+1} = \lambda_{Az}^k + \alpha_{Az} (z_{0A}^{k+1} - z_{1A}^{k+1}) \quad (21)$$

$$\lambda_{Bz}^{k+1} = \lambda_{Bz}^k + \alpha_{Bz} (z_{0B}^{k+1} - z_{1B}^{k+1}) \quad (22)$$

For each of the four OPFs, the same system constraints as in a standard OPF still hold.

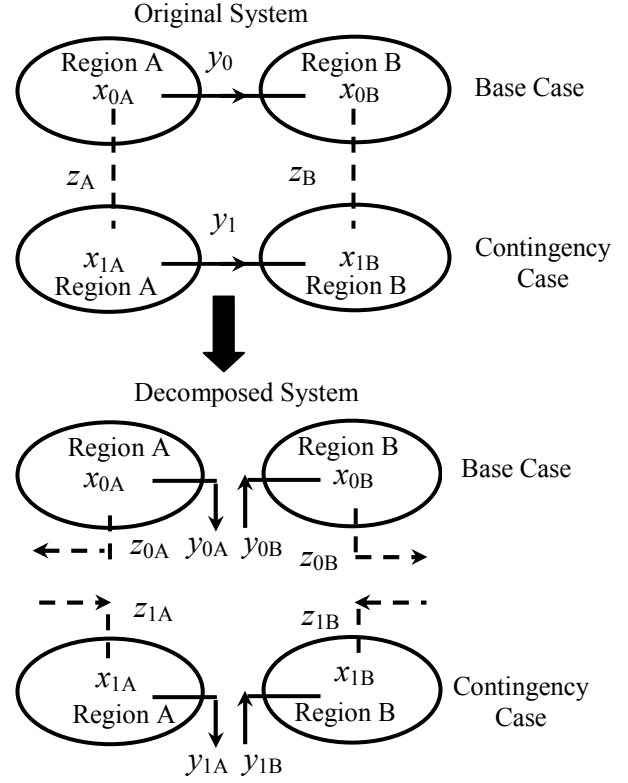


Figure 3. Example of DCAS decomposition

### 3. Energy Pricing and Opportunity Cost

#### 3.1. Locational Marginal Pricing (LMP)

The economic rationale for applying marginal cost pricing to an electricity network using the concepts of LMP was presented in [13]. LMP in electricity recognizes that the marginal price may differ at different locations and times. Differences result from transmission congestion and transmission losses. LMP is believed to be an efficient market-based method for transmission congestion control and was also recommended in the SMD NOPR. Currently, LMP is being used in the PJM and NYISO energy markets. And other ISOs, like ISO-New England and CAISO, also propose to adopt LMP in the near future.

As explained in [9-10], the pricing structure is based on an *Augmented OPF (AOPF)* which adds reserves to the standard OPF. The *Unit Committed Generation Intervals*  $[G_i^{\min}, G_i^{\max}]$  obtained from the CO-OPT are carried on to the AOPF to replace the actual physical generation limits for each of the generators.

Assume  $\lambda_j$  is the Lagrange multiplier associated with nodal real power balancing at bus  $j$  from the AOPF;  $\mu_{G_i^{\min}}$  and  $\mu_{G_i^{\max}}$  ( $i=1,2,\dots,I$ ) are the Lagrange multipliers from the AOPF related to the upper and lower

boundaries of the *Unit Committed Generation Intervals*. Define

$$\alpha_{ij} = \frac{\Delta G_i^{\min}}{\Delta D_j} \quad (23)$$

$$\beta_{ij} = \frac{\Delta G_i^{\max}}{\Delta D_j} \quad (24)$$

where  $D_j$  is the real load at bus  $j$ .  $\alpha_{ij}$  is the sensitivity of change of  $G_i^{\min}$  with respect to the change of bus  $j$  load, that is, if there is one unit of load variation at bus  $j$ ,  $\alpha_{ij}$  indicates the corresponding shift of  $G_i^{\min}$ .  $\beta_{ij}$  has similar definition for  $G_i^{\max}$ . The nodal energy price at bus  $j$ ,  $\bar{\lambda}_j$ , then can be calculated as

$$\bar{\lambda}_j = \lambda_j + \sum_{i=1}^I (\alpha_{ij} \mu_{G_i^{\min}} + \beta_{ij} \mu_{G_i^{\max}}), \quad j=1, \dots, J \quad (25)$$

The subtlety of this equation is explained in [9-10] and the method used to compute  $\alpha_{ij}$  and  $\beta_{ij}$  is provided in Appendix B.

### 3.2. Opportunity Cost (OC) Payment for Ancillary Services

We demonstrated in [10] by testing a joint energy-reserve market, paying reserves the OC of forgone profits for energy is a promising way to mitigate speculative behavior compared to paying separate prices for energy and reserves.

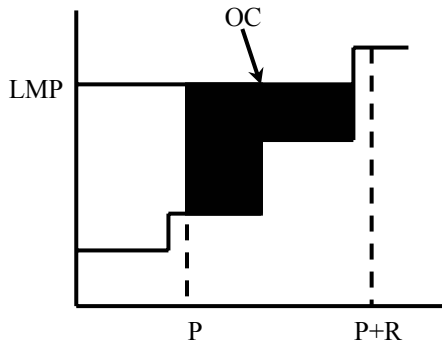


Figure 4. Illustration of OC computation

The OC is equal to the product of: (1) the quantity of reserves provided and (2) the price difference between (a)

the LMP existing at the time the generator was instructed to provide reserves and (b) the generator's energy offer for the same MW segment. Fig. 4 illustrates how the OC is calculated. Payment of OC for the reserves actually makes it indifferent, in the sense of profit-making, for the seller to supply energy or reserves, thus encouraging electricity suppliers to offer enough reserve capacity into the market. Also, notice in Fig. 4 that suppliers have the risk of providing free reserves if their energy offers are too high, thus discouraging speculative behavior.

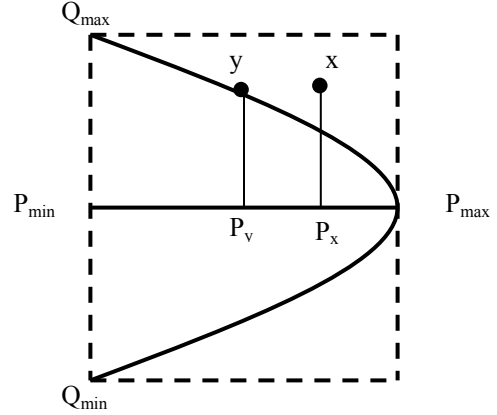


Figure 5. Generator capability curve

The same idea can be extended to another important ancillary service, VAR support. To simplify the formulation for a standard OPF, the generation limits are usually modeled as boxes (dashed lines) as shown in Fig.5. However, to be more precise, the active and reactive power outputs of a generator cannot be freely determined. They are actually limited by certain generator characteristics, namely *generator capability curves*. They have the shape of the solid curve in Fig.5. The region enclosed by the curve is the feasible output region for the generator. The dispatch difference with or without the capability curve is illustrated in Fig.5. With the box constraint, the generator would be dispatched at the point  $x$ . With the capability curve, however, assume the VAR support from this generator is essential, then the generator would have to be backed off and dispatched at point  $y$ . This scenario explains that the generator loses profit on energy for providing VAR support for the network. Similarly, the OC payment can be paid to the generator compensating for its forgone profit on energy. In particular, the OC payment can be calculated as in Fig. 4 but with  $P$  and  $(P+R)$  replaced by  $P_y$  and  $P_x$  respectively.

Two OPFs, with and without capability curves respectively, are needed for computing the OC for VAR support. Therefore, in analogy, when considering the OC payment for both reserves and VAR support, two CO-OPTs with and without capability curves are also needed. In this case, for the OC calculation in Fig.4, 'P' would be

the dispatch given the current state of nature with the consideration of capability curves, and 'P+R' would be replaced by the maximum dispatch over all contingencies without capability curves.

#### 4. A Simple Demonstration

The DCAS is implemented in Matlab. The solutions to the sub-problem OPFs are solved by a Matlab build-in function 'fmincon'. And it is not a really distributed implementation, but a mimic by an iterative serial computation. We are in the very early stage of the algorithm development, hence, the focus here is on the validity rather than the efficiency of the proposed decomposition scheme. Efficiency related problems, such as a high-performance OPF solver and parallel implementation, will be our next step.

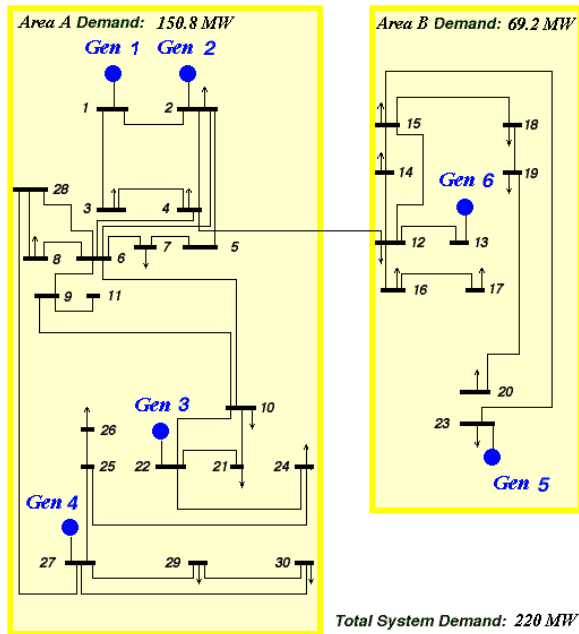


Figure 6. Modified IEEE 30-bus test system

The validity of the proposed coordination scheme is tested using a modified IEEE 30-bus system shown in Fig. 6. The overall system is divided into two control areas with one tie-line connecting each other. There are 4 generators in area A and 2 generators in area B. Each of the generators has a maximum capacity of 60 MW. Suppose that two ISOs manage the two areas respectively. And also assume their market designs and rules are similar enough to be able to trade energy and ancillary services across the boundary with no barriers. A small amount of boundary information is exchanged between two areas in a timely fashion. The market mimicking here is in a one-market set-up with fixed demand. Suppliers

submit only energy offers to the market. The ISOs clear the market based on the DCAS framework, pay energy nodal prices and ancillary services opportunity costs. The offer curves are piecewise-linear.

For simplicity, the DCAS coordinates energy and spinning reserves only, and is set up for the situation of one base case and one contingency. The base case is set to be the intact system as shown in Fig. 6. And the contingency case is the lost of Gen # 2 in area A. The probabilities for each case to happen are 80% and 20%. The overall system is also solved in a centralized fashion to validate the results via the decentralized procedure.

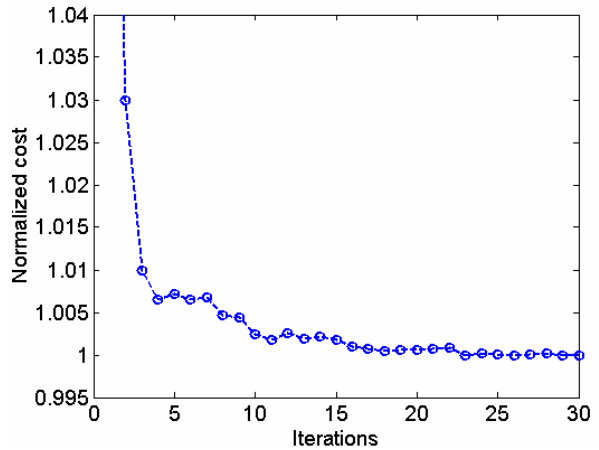


Figure 7. Normalized total cost evaluation vs. iterations in DCAS implementation

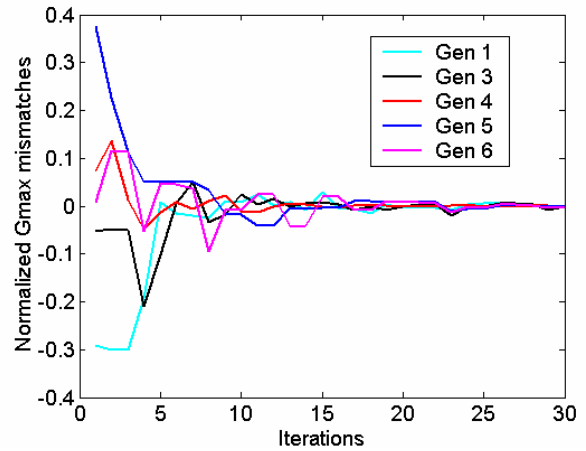


Figure 8. Normalized Gmax (TUCC) mismatches vs. iterations in the DCAS implementation

Fig. 7 shows the evaluation of total cost for the DCAS implementation as a function of the number of iterations. The costs in Fig.7 are normalized with respect to the optimum cost got in the centralized way. Fig. 8 shows the

convergence pictures of TUCCs between the base case and the contingency case (also normalized with respect to centralized results). The convergence of the boundary “dummy” variables between areas is in a similar fashion. Therefore, for this particular system, it takes 30 iterations to converge. The stopping criterion is chosen to be 0.03 per unit maximum mismatch as suggested by Kim and Baldick [5-7]. But typically, most of the mismatches are much smaller than 0.03 per unit as seen in Fig. 8. The total cost obtained on this stopping criterion was also reported by Kim and Baldick to be within 0.1% of the optimal production cost. Our result of Fig.7 is consistent with their observations.

Table 1. An example of base dispatches and prices by DCAS vs. centralized CO-OPT computation

Gen #	Base Dispatch (MW)		Base Energy Price (\$/MWh)	
	Distributed	Central	Distributed	Central
1	36.00	36.00	48.45	48.57
2	36.00	36.00	48.90	49.02
3	36.00	36.00	48.68	48.90
4	36.00	36.00	49.13	49.31
5	43.51	43.53	49.00	49.00
6	36.00	36.00	48.81	48.93

Table 1 lists the final dispatches and prices obtained through the distributed procedure. These numbers are also compared to the results via the centralized optimization. The small errors are due to the 0.03 per unit convergence tolerance. If a smaller tolerance were chosen, smaller errors would be expected.

Basically, the DCAS results for this particular example are consistent with Kim and Baldick’s experience for small systems.

## 5. Discussions and Conclusions

We proposed in this paper a distributed process for simultaneously coordinating interchanges of energy, spinning reserves and VAR support between multiple areas. The algorithm does not require a common control center. It is sufficient for involved areas to follow certain rules and exchange a small amount of boundary information. The theoretical framework was introduced. And a simple example based on a modified IEEE 30-bus system justified its validity. The proposed coordination approach preserves dispatching independence for each of neighboring ISOs while achieves a multi-area optimum. The algorithm is of particular interest in resolving seams issues.

Another motivation for this approach is that the method would get close to the optimum solution fairly quickly, otherwise it would be of little use to real implementation. However, the implementation efficiency problem was not addressed in this paper. A system of 30 buses is too small to be realistic. And the Matlab implementation is for the sole purpose of demonstration also. Nevertheless, Kim and Baldick’s happy convergence experience<sup>1</sup> with the same decomposition principle seems to suggest that good early convergence in our DCAS formulation for real-size systems may be a viable conjecture. To build an efficient OPF solver and to do a real parallel processing will be an important next step.

Our previous work [9-10] showed that the joint energy-reserve market based on the CO-OPT has better market performance and economic efficiency than the existing form of market with fixed reserve requirements. And the OC payment for reserves is a promising way to alleviate speculative behavior. The optimization framework and the payment mechanism are extended to another ancillary services, VAR support, which is also a key element for reliable transmission services. In the existing electricity markets, VAR support service is mainly arranged by contracts rather than the market itself. Although we have not done any serious tests of markets with OC payments for VAR support, the way of including VAR support in the optimization and paying the corresponding OC is a promising approach to compensating suppliers for the actual service provided. In contrast, trying to establish a separate market for VARs would probably create problems of market power that are even more serious than they are in existing fixed reserve markets.

## 6. Acknowledgements

This work was supported in part by the US Department of Energy through the Consortium for Electric Reliability Technology Solutions (CERTS) and in part by the National Science Foundation Power Systems Engineering Research Center (PSERC).

## 7. References

<sup>1</sup> They reported in their work [5], “For some small systems, including the 50 bus system ..., required over 20 iterations. However, for larger systems, including the two ERCOT systems, ... required no more than five iterations to satisfying the stopping criterion”; “almost all of the potential production cost savings are achieved within 3 or 4 iterations”.

[1] Seams Issues – High Priority Items, [online]: [http://www.isomou.com/working\\_groups/business\\_practices/documents/general/bpwg\\_matrix.pdf](http://www.isomou.com/working_groups/business_practices/documents/general/bpwg_matrix.pdf)

[2] IMO of Ontario, ISO-NE and NYISO Complete Planning and Market Development Agreement, [online]: [http://www.theimo.com/imoweb/pubs/pressReleases/pr\\_NYISO-ISON-IMO\\_20020717.pdf](http://www.theimo.com/imoweb/pubs/pressReleases/pr_NYISO-ISON-IMO_20020717.pdf)

[3] Northeast ISOs Seams Resolution Report: History of Seam Issues Resolution, [online]: <http://www.iso-ne.com/FERC/seams/NESeamsDetListing011503.pdf>

[4] S.Harvey, “Proxy Buses, Seams and Markets [Draft]”, May, 23, 2003, [online]: [http://www.ksg.harvard.edu/hepg/Papers/Harvey\\_Proxy.Buses.Seams.Markets\\_5-23-03.pdf](http://www.ksg.harvard.edu/hepg/Papers/Harvey_Proxy.Buses.Seams.Markets_5-23-03.pdf)

[5] B.H. Kim and R. Baldick, “Coarse-Grained Distributed Optimal Power Flow”, *IEEE Trans. On Power Systems*, v12 n2, May, 1997, p932-939

[6] R. Baldick, B.H. Kim, C. Chase, and Y. Luo, “A Fast Distributed Implementation of Optimal Power Flow”, *IEEE Trans. On Power Systems*, v14 n3, Aug. 1999, p858-864

[7] B.H. Kim and R. Baldick, “A Comparison of Distributed Optimal Power Flow Algorithms”, *IEEE Trans. On Power Systems*, v15 n2, May, 2000, p599-604

[8] M.D. Cadwalader, S.M. Harvey, S.L. Pope and W.W. Hogan, “Market Coordination of Transmission Loading Relief Across Multiple Regions”, Dec. 1998, [online]: <http://ksghome.harvard.edu/~whogan.cb.g.Ksg/extr1298.pdf>

[9] J.Chen, T.D. Mount, J.S. Thorp, R.J. Thomas, “Location-based Scheduling and Pricing for Energy and Reserves: A Responsive Reserve Market Proposal”, submitted to *special issue on Competitive Electricity Market of Journal of Decision Support Systems*

[10] J.Chen, J.S. Thorp, R.J. Thomas, and T.D. Mount, “Locational Pricing and Scheduling for An Integrated Energy-Reserve Market”, 36<sup>th</sup> Hawaii International Conference on System Science, Hawaii, Jan. 2003

[11] A.J. Wood and B.F. Wollenberg, *Power Generation, Operation and Control*, John Wiley & Sons Inc., New York, 1996

[12] G. Cohen, “Auxiliary Problem Principle and Decomposition of optimization problems”, *Journal of Optimization Theory and Applications*, v32 n3, Nov. 1980, p277-305

[13] F.C. Schweppe, M.C. Caraminis, R.D., Tabors, and R.E. Bohn, *Spot Pricing of Electricity*, Kluwer Academic Publishers, 1988

[14] G.P. McCormick, *Nonlinear Programming: Theory, Algorithms, and Applications*, Wiley, New York, 1983

## Appendix

### A. General APP-based Decomposition Formulation

Consider a general optimization problem of the form

$$\begin{aligned} \min \sum_{i=1}^n f_i(x_i) \\ \text{s.t.} \quad h_i(x_i) = 0, \quad i = 1, 2, \dots, n \\ g_i(x_i) \leq 0, \quad i = 1, 2, \dots, n \\ \sum_{i=1}^n A_i x_i = 0 \end{aligned} \quad (\text{A.1})$$

where every  $f_i$  is convex and has a derivative that obeys a Lipschitz condition. Based on APP[12], solving problem (A.1) is equivalent to iteratively solve the following sub-problems, for  $i = 1, \dots, n$

$$\begin{aligned} x_i^{k+1} = \min \left\{ f_i(x_i) + \frac{\beta}{2} \|x_i - x_i^k\|^2 \right. \\ \left. + (\lambda^k)^T \cdot (A_i x_i) + \gamma \cdot \sum_{j=1}^n (A_j x_j^k)^T \cdot (A_i x_i) \right\} \\ \text{s.t.} \quad h_i(x_i) = 0 \\ g_i(x_i) \leq 0 \end{aligned} \quad (\text{A.2})$$

$$\lambda^{k+1} = \lambda^k + \alpha \cdot \sum_{j=1}^n (A_j x_j^k) \quad (\text{A.3})$$

In particular, for power systems, problem (A.1)~(A.3) can be formulated for a multi-region OPF, a single-region CO-OPT, or a multi-region CO-OPT, as described in the paper.

### B. Computation of $\alpha_{ij}$ and $\beta_{ij}$

The computation of  $\alpha_{ij}$  and  $\beta_{ij}$  is actually a standard problem of sensitivity analysis in nonlinear programming [14]. Consider a general sensitivity problem written as

$$\begin{aligned} \min f(x, \varepsilon) \\ \text{s.t.} \quad h_i(x, \varepsilon) = 0, \quad i = 1, 2, \dots, m \\ g_j(x, \varepsilon) \leq 0, \quad j = 1, 2, \dots, n \end{aligned} \quad (\text{B.1})$$

where  $\varepsilon$  is a vector of parameters. Loosely speaking, the solution can be regarded as a function of  $\varepsilon$ , denoted by  $x(\varepsilon)$ . The problem of interest is how does the solution change as  $\varepsilon$  changes.

Assume the functions in (B.1) are twice continuously differentiable with respect to  $x$  and  $\varepsilon$ . Let  $(x_0, \lambda_0, \mu_0) = [x(\varepsilon_0), \lambda(\varepsilon_0), \mu(\varepsilon_0)]$  be a KKT triple satisfying the first-order optimality conditions

$$\left\{ \begin{array}{l} L(x_0, \lambda_0, \mu_0, \varepsilon_0) = \nabla f(x_0, \varepsilon_0) + \sum_{i=1}^m \nabla h_i(x_0, \varepsilon_0) \cdot \lambda_0^i \\ \quad + \sum_{j=1}^n \nabla g_j(x_0, \varepsilon_0) \cdot \mu_0^j = 0 \\ \mu_0^j \cdot g_j(x_0, \varepsilon_0) = 0, \quad j = 1, 2, \dots, n \\ h_i(x_0, \varepsilon_0) = 0, \quad i = 1, 2, \dots, m \end{array} \right. \quad (\text{B.2})$$

Let  $Y_0 = (x_0, \lambda_0, \mu_0)$  and define

$$G(Y_0, \varepsilon_0) = \left[ \begin{array}{l} L(x_0, \lambda_0, \mu_0, \varepsilon_0) \\ \mu_0^j \cdot g_j(x_0, \varepsilon_0) = 0, j = 1, 2, \dots, n \\ h_i(x_0, \varepsilon_0) = 0, i = 1, 2, \dots, m \end{array} \right] = 0 \quad (\text{B.3})$$

For  $\varepsilon = \varepsilon_0 + \Delta\varepsilon$  in a neighborhood of  $\varepsilon_0$ , at the new optimum, by KKT conditions,

$$G(Y_0 + \Delta Y, \varepsilon_0 + \Delta\varepsilon) = 0 \quad (\text{B.4})$$

Ignore the high-order terms,

$$\begin{aligned} G(Y_0 + \Delta Y, \varepsilon_0 + \Delta\varepsilon) &= G(Y_0, \varepsilon_0) \\ &+ \frac{\partial G}{\partial Y} \cdot \Delta Y + \frac{\partial G}{\partial \varepsilon} \cdot \Delta\varepsilon \end{aligned} \quad (\text{B.5})$$

Substitute (B.3) and (B.4) into (B.5),

$$\frac{\Delta Y}{\Delta\varepsilon} = \begin{bmatrix} \frac{\Delta x}{\Delta\varepsilon} \\ \frac{\Delta\lambda}{\Delta\varepsilon} \\ \frac{\Delta\mu}{\Delta\varepsilon} \end{bmatrix} = - \left[ \frac{\partial G}{\partial Y} \right]^{-1} \cdot \left[ \frac{\partial G}{\partial \varepsilon} \right] \quad (\text{B.6})$$

$\frac{\partial G}{\partial Y}$  and  $\frac{\partial G}{\partial \varepsilon}$  are evaluated at  $Y_0$  and  $\varepsilon_0$  respectively.

Their detailed formulation and the rigorous proof of (B.6) are referred to [14].

As a specific example of computing  $\alpha_{ij}$  and  $\beta_{ij}$  defined in Section 2.6, (B.1) is formulated as the CO-OPT, and  $\varepsilon$  is taken as the vector of nodal real power demand.  $\alpha_{ij}$  and  $\beta_{ij}$  then can be extracted from  $\frac{\Delta x}{\Delta\varepsilon}$  in (B.6). If the DCAS problem of form (A.2) is solved, the computation of  $G(Y_0, \varepsilon_0)$  should also include the consistency constraints, expressed in the overall problem (A.1), which force all copies of duplicated variables to be equal.